Submission and Issues available at dergipark.gov.tr

KARADENIZ CHEMICAL SCIENCE AND TECHNOLOGY

Journal web page: www.kcstjournal.org

Research Article

Peripherally tetra 1,2,4-triazole substituted novel phthalocyanines: synthesis, characterization, electrochemical and spectroelectrochemical properties

Ayşe Aktaş Kamiloğlu[1,*], Mehmet Aydemir[2], İrfan Acar[3], Gülbınar Sarkı[4], Atıf Koca[2], Nurhan Gümrükçüoğlu[5], Ümmühan Ocak[4], Halit Kantekin[4]

[1] *Artvin Vocational School, Artvin Çoruh Universty, 08100 Artvin, Turkey*
[2] *Department of Chemical Engineering, Engineering Faculty, Marmara University, 34722 Göztepe, Istanbul, Turkey*
[3] *Department of Energy Systems Engineering, Of Faculty of Technology, Karadeniz Technical University, 61830 Of, Trabzon, Turkey*
[4] *Department of Chemistry, Faculty of Science, Karadeniz Technical University, 61080 Trabzon, Turkey*
[5] *Vocational School of Health Services, Karadeniz Technical University, 61080 Trabzon, Turkey*

Keywords:
phthalocyanines,
oxygen reduction reaction,
spectroelectrochemistry,
electrosensor,
titanium

ABSTRACT

In this study, the synthesis, electrochemical and spectroelectrochemical properties of new peripherally 1,2,4-triazole substituted metal-free **4**, Zn(II) **5**, Ti(IV) **6,** Ni(II) **7** and Co(II) **8** phthalocyanine derivatives were reported. Voltammetric and in situ spectroelectrochemical characterization of the complexes were performed in solution. Since nickel and zinc phthalocyanines gave common phthalocyanine ring based electron transfer reactions with the characteristic "energy gaps", "peak to peak potential separations" and "half wave peak potential values", Co^{II} and $Ti^{IV}O$ metal ions behaved as redox active cations in the core of the cobalt and titanium phthalocyanine complexes, respectively. While cobalt phthalocyanine gave a one-electron $[Co^{II}Pc^{-2}]/[Co^{I}Pc^{-2}]^{-1}$ reduction reaction, titanium phthalocyanine illustrated two metal based reduction reactions, $[Ti^{IV}OPc^{-2}]/[Ti^{III}OPc^{-2}]^{-1}$ and $[Ti^{III}OPc^{-2}]^{-1}/[Ti^{III}OPc^{-2}]^{-2}$, in addition to the Pc ligand reduction processes. Electron transfer reactions altered the spectra of the complexes considerably, which is one of the most important expectations for the practical applications of the complexes especially in display technologies. Redox and spectral responses of cobalt and titan complexes were affected by the molecular oxygen present in the electrolyte, which indicates electrocatalytic and electrosensing activity of the complexes towards the molecular oxygen.

TR

Periferal tetra 1,2,4,-triazol sübstitüe yeni ftalosiyaninler: sentez, karakterizasyon, elektrokimyasal ve spektroelektrokimyasal özellikler

Anahtar Kelimeler:
Ftalosiyanin,
oksijen indirgenme reaksiyonu,
spektroelektrokimya,
elektrosensör,
titanyum

ÖZET

Bu çalışmada, yeni peripheral 1,2,4-triazol substitue metalsiz **4**, Zn(II) **5**, Ti(IV) **6,** Ni(II) **7** ve Co(II) **8** ftalosiyanin türevlerinin sentezi, elektrokimyasal ve spektroelektrokimyasal özellikleri rapor edilmiştir. Komplekslerin voltametrik ve in situ spektroelektrokimyasal karakterizasyonu çözelti içinde gerçekleştirildi. Nikel ve çinko ftalosiyaninler karakteristik olarak ortak "enerji aralığı"," pikten pike potansiyel ayrımlar" ve "yarım dalga pik potansiyel değerleri" ile ftalosiyanin halka bazlı elektron transfer reaksiyonu verirken, kobalt ve titanyum ftalosiyanin komplekslerinin kavitesinde bulunan Co^{II} ve $Ti^{IV}O$ metal iyonları redoks aktif katyon olarak davranmıştır. Kobalt ftalosiyanin indirgenme reaksiyonunda bir elektron $[Co^{II}Pc^{-2}]/[Co^{I}Pc^{-2}]^{-1}$ verirken, titanyum ftalosiyanin Pc ligand indirgenme işlemine ek olarak, iki tane metal bazlı indirgenme reaksiyonu $[Ti^{IV}OPc^{-2}]/[Ti^{III}OPc^{-2}]^{-1}$ ve $[Ti^{III}OPc^{-2}]^{-1}/[Ti^{III}OPc^{-2}]^{-2}$ göstermiştir. Elektron transfer reaksiyonları komplekslerin spektrumlarını oldukça değiştirmiştir. Bu durum komplekslerin özellikle görüntüleme teknolojisinde pratik uygulamalarda en önemli beklentidir. Kobalt ve titanyum komplekslerinin redoks ve spektral yanıtları elektrolitte var olan moleküler oksijen tarafından etkilenmiştir. Bu da komplekslerin moleküler oksijene karşı elektrokatalitik ve elektosensör aktivitesini göstermektedir.

1. Introduction

Phthalocyanines (Pcs), which were discovered as first industrial pigments, have played role in wide study of fields such as photocopying, optical recording, gas sensing, photovoltaics, liquid crystals, oxidation catalysts, chemical sensors, photovoltaic solar cells and photodynamic therapy (PDT). They also have good thermal and chemical stability and visible area optical properties thanks to having strong 18π-electron delocalization [1-6].

In recent years, many axially substituted phthalocyanine complexes have been synthesized to increase solubility. In many cases, applications of phthalocyanine depend on their solubility. But, it is vitally important to control the aggregation behaviors of Pcs. Aggregation decreases their solubility and minimizes their applications in many organic solvents [7].

On the other hand, widespread and successful applications of heteroaromatic ring are to participate in various interactions due to its

*Corresponding author: ayse_ aktas_kamiloglu@artvin.edu.tr
Citation: Aktaş Kamiloğlu, A., Aydemir, M., Acar, İ., Sarkı, G., Koca, A., Gümrükçüoğlu, N., Ocak, Ü., Kantekin, H., Peripherally tetra 1,2,4-triazole substituted novel phthalocyanines: synthesis, characterization, electrochemical and spectroelectrochemical properties, *Karadeniz Chem. Sci. Tech.* 2017, 1, 22-30.
DOI:
ISSN:

high resistance to metabolic degradation and ability, such as Van der Waals and ione dipole interactions, hydrogen and coordination bonds, cation-π and π-π stackings in biological systems [8]. N-bridged heterocyclic derivatives that derived from 1,2,4-triazoles show several biological activities as antimicrobial, anticancer, analgesic, sun-protective, antiviral, anti-inflammatory, antitumor, anti HIV, anti fungal and anticonvulsants properties [9,10].

Tailoring various substituents to the periphery and/or nonperiphery of phthalocyanines and different metal centers in the core of the Pc ring alter the redox activity of the complexes [11]. Each new complex may have extraordinary redox behaviors due to the effect of new substituents and metal centers. For this reason, electrochemical behavior of a newly synthesized complex should be determined to decide their possible application fields with respect to the electrochemical responses. Thus, we have investigated the electrochemical and spectroelectrochemical features of the MPc complexes synthesized.

In this work, novel phthalocyanine derivatives bearing 1,2,4-triazole groups have been synthesized. The structures of the new compounds were characterized by IR, ^{1}H-NMR, ^{13}C-NMR, UV–Vis and mass spectroscopic data. In addition, aggregation behavior of metal-free- and Zn-phthalocyanines were investigated in different solvents, and their different concentrations were studied in $CHCl_3$.

2. Experimental

2.1. Materials

The used materials, equipments and electrochemical procedure were supplied as Supporting Information (SI).

2.2. Synthesis

2.2.1. Synthesis of 4-[2-((E)-{[3-(4-methylphenyl)-5-phenyl-4H-1,2,4-triazol-4-yl]imino}methyl)phenoxy]-phthalonitrile (3)

4-Nitrophthalonitrile (**2**) (0.73 g, 4.23x10^{-3} mol) was dissolved in 0.01 L of dry DMF under N_2 atmosphere, and 2-((E)-{[3-(4-methylphenyl)-5-phenyl-4H-1,2,4-triazol-4-yl]imino}methyl)phenol (**1**) (1.5 g, 4.23x10^{-3} mol) was added to reaction mixture. After stirring for 30 min at 60 °C, finely ground anhydrous K_2CO_3 (1.75 g, 12.69 x10^{-3} mol) was added portion wise during 2 h. The reaction mixture was stirred under N_2 at 60 °C for 4 days. The reaction progress was monitored by thin layer chromatography (TLC) using chloroform as a solvent. After this time, the reaction mixture was poured into ice-water and stirred at room temperature for 3 h to yield a crude product. The mixture was filtered and washed with water, then dried in vacuum over P_2O_5 for 4 h, and recrystallized from ethanol to give light yellow crystalline powder. Yield: 1.1 g (53%). mp: 120-121 °C. IR (KBr pellet), ν_{max}/cm^{-1}: 3070 (Ar-H), 2965-2857 (Aliph. C-H), 2233 (C≡N), 1602-1565 (C=N), 1482-1446 (C=C), 1277-1251 (Ar-O-Ar), 1158-1102 (C-N), 950, 774, 525. ^{1}H-NMR. ($CDCl_3$), (δ:ppm): 8.33 (d, 1H, J=9.2 Hz, =C-H), 8.19 (dd, 1H, J=8.0 Hz, Ar-H), 8.07 (m, 1H, Ar-H), 7.97 (d, 1H, J=8.4 Hz, Ar-H), 7.78-7.57 (m, 5H, Ar-H), 7.31-7.25 (m, 3H, Ar-H), 7.16-7.01(m, 3H, Ar-H), 6.99-6.86 (m, 2H, Ar-H), 2.32 (d, 3H, J=8.4 Hz, -CH_3). ^{13}C-NMR. ($CDCl_3$), (δ:ppm): 170.33, 161.72, 160.48, 159.85, 153.43, 140.43, 140.23, 135.55, 135.35, 132.39, 130.13, 129.86, 129.69, 129.47, 128.96, 128.61, 128.52, 128.42, 127.12, 123.95, 123.34, 121.40, 121.09, 120.12, 117.64, 115.99(C≡N), 115.06(C≡N), 114.66, 22.67. MS (ESI), (m/z): Calculated: 480.53; Found: 481.37 $[M+H]^+$ (Fig. S1, SI).

2.2.2. Synthesis of metal-free phthalocyanine (4)

A mixture of phthalonitrile **3** (0.2 g, 0.42x10^{-3} mol) and 1.8-diazabicyclo[5.4.0]undec-7-ene (DBU) (5 drop) in 0.0025 L of dry n-amyl alcohol was heated and stirred at 160 °C in a sealed glass tube for 16 h under N_2. After cooling to room temperature, the green crude product was precipitated with ethanol, filtered and washed with ethanol, then diethyl ether, and then dried in vacuo. Finally, pure metal-free phthalocyanine was obtained by column chromatography using basic aluminium oxide and $CHCl_3$:CH_3OH (25:1) as solvent system. Yield: 0.040 g (20%). mp: > 300 °C. IR (KBr tablet) ν_{max}/cm^{-1}: 3292 (N-H), 3066 (Ar-H), 2960-2851 (Aliph. C-H), 1599-1575 (C=N), 1484-1446 (C=C), 1235 (Ar-O-Ar), 1090-1011 (C-N), 928, 828, 740. ^{1}H-NMR. ($CDCl_3$), (δ:ppm): 8.08 (m, 4H, =C-H), 7.42 (m, 30H, Ar-H), 7.32- 6.94 (m, 34H, Ar-H), 1.70 (m, 12H, -CH_3). UV-Vis ($CHCl_3$): λ_{max}, nm (log ε): 698 (4.99), 664 (4.93), 644 (4.63), 607 (4.46), 342 (4.92). MALDI-TOF-MS, (m/z): Calculated: 1924.09; Found: 986 [M- 4($C_{15}H_{12}N_3$)]$^+$.

2.2.3. Zinc(II) phthalocyanine (5)

A mixture of phthalonitrile **3** (0.3 g, 0.62x10^{-3} mol) and anhydrous metal salt $Zn(CH_3COO)_2$ (0.058 g, 0.31x10^{-3} mol) and 1.8-diazabicyclo[5.4.0]undec-7-ene (DBU) (4 drop) in 0.0025 L of dry n-amyl alcohol was heated and stirred at 160 °C in a sealed glass tube for 16 h under N_2. After cooling to room temperature, a precipitate was formed by the addition of ethanol, and green precipitate was filtered off. The obtained green product was washed with ethanol and diethyl ether and then dried in vacuo. Purification of the solid product was accomplished by column chromatography using basic aluminium oxide and $CHCl_3$:CH_3OH (5:1) as solvent system. Yield: 0.076 g (25%). mp: >300 °C. IR (KBr tablet) ν_{max}/cm^{-1}: 3058 (Ar-H), 2927-2857 (Aliph. C-H), 1599-1576 (C=N), 1483-1446 (C=C), 1238 (Ar-O-Ar), 1086-1044 (C-N), 943, 893, 740. ^{1}H-NMR. ($CDCl_3$), (δ:ppm): 7.79 (m, 4H, =C-H) , 7.53 (m, 30H, Ar-H), 7.44-6.70 (m, 34H, Ar-H), 1.52 (m,12H, -CH_3) (Fig. S2, SI). UV-Vis ($CHCl_3$): λ_{max}, nm (log ε): 677 (4.97), 611 (4.35), 351 (4.69). MALDI-TOF-MS,(m/z): Calculated: 1987.45; Found: 1050.38 [M-4($C_{15}H_{12}N_3$)]$^+$ (Fig. S3, SI).

2.2.4. Ti(IV) phthalocyanine (6)

A mixture of compound **3** (0.15 g, 0.31x10 $^{-3}$ mol) and 1,8-diazabycyclo[5.4.0]undec-7-ene (DBU) (4 drop) was mixed in 0.0015 L dry n-amyl alcohol and heated to 120 °C. At that temperature, anhydrous titanium (IV) butoxide $Ti(OBu)_4$ (0.00011 L) was added through a syringe, and the reaction mixture was heated under reflux at 160 °C for 12 h. After cooling to room temperature, the mixture was poured into n-hexane and stirred for 5 h. Then dark green product was filtered and then washed with hot diethyl ether and dried in vacuum over P_2O_5. Purification of the solid product was accomplished by column chromatography using basic aluminium oxide and $CHCl_3$:CH_3OH (5:1) as solvent system. Yield: 0.090 g (15%). mp: >300 °C. IR (KBr tablet) ν_{max}/cm^{-1}: 3071 (Ar-H), 2919-2850 (Aliph. C-H), 1599-1575 (C=N), 1472-1446 (C=C), 1237 (Ar-O-Ar), 1070 (C-N), 944, 830, 747. ^{1}H-NMR. ($CDCl_3$), (δ:ppm): 8.12 (m, 4H, =C-H), 7.89 (m, 24H, Ar-H), 7.88-7.50 (m, 32 H, Ar-H), 7.40-7.23 (m, 8H, Ar-H), 1.54 (m, 12H, -CH_3), UV-Vis ($CHCl_3$): λ_{max}, nm (log ε): 698 (5.06), 666 (4.56), 631 (4.44), 349 (4.76). MALDI-TOF-MS, (m/z): Calculated: 1985.98; Found: 1049.56 [M-4($C_{15}H_{12}N_3$)]$^+$.

2.2.5. Nickel(II) phthalocyanine (7)

Synthesized similarly to **5** from **3** by using anhydrous $NiCl_2$. Yield: 0.043 g (41%). mp: > 300 °C. IR (KBr tablet) ν_{max}/cm^{-1}: 3052 (Ar-H), 2926-2873 (Aliph. C-H), 1598-1575 (C=N), 1470-1446 (C=C), 1235 (Ar-O-Ar), 1090-1060 (C-N), 956, 879, 748. ^{1}H-NMR. ($CDCl_3$), (δ:ppm): 7.45 (m, 4H, =C-H), 7.18 (m, 64H, Ar-H), 1.58 (m, 12H, -CH_3). UV-Vis ($CHCl_3$): λ_{max}, nm (log ε): 668 (5.02), 621 (4.86), 334 (4.93). MALDI-TOF-MS, (m/z): Calculated: 1980.78; Found: 1042.78 [M- 4($C_{15}H_{12}N_3$)]$^+$ (Fig. S4, SI).

2.2.6. Cobalt (II) phthalocyanine (8)

Synthesized similarly to **5** from **3** by using anhydrous $CoCl_2$. Yield: 0.015 g (15%). mp: > 300 °C. IR (KBr tablet) ν_{max}/cm^{-1}: 3053 (Ar-H), 2922-2859 (Aliph. C-H), 1575-1598 (C=N), 1467-1446 (C=C), 1235 (Ar-O-Ar), 1091 (C-N), 957, 879, 750. UV-Vis ($CHCl_3$): λ_{max}, nm (logε): 670 (5.03), 640 (4.85), 346 (5.00). MALDI-TOF-MS, (m/z): Calculated: 1981.01; Found: 1044.25 [M- 4($C_{15}H_{12}N_3$)]$^+$ (Fig. S5, SI).

3. Results and discussion

3.1. Outlook of the synthesized compounds

The general synthetic route for the synthesis of new metal-free and metallophthalocyanines that starts form 2-((*E*)-{[3-(4-methylphenyl)-5-phenyl-4*H*-1,2,4-triazol-4-yl]imino}methyl)phenol **1** [12] and 4-nitrophthalonitrile **2** is summarized in Fig. 1. The structures of the new compounds were characterized by using an assembly of UV-Vis (for **4**-**8**), IR, ^{1}H-NMR (for **3**-**7**), ^{13}C-NMR and MS spectral data.

3.2. Synthesis and characterization

The synthesis of compound **3** was based on the reaction of 2-((E)-{[3-(4-methylphenyl)-5-phenyl-4H-1,2,4-triazol-4-yl]imino}methyl)phenol **1** with 4-nitrophthalonitrile **2** (in dry DMF and in the presence of dry K_2CO_3 as base, at 60 °C in 96 h). The formation of compound **3** was confirmed by the combination of spectroscopic data. In the IR spectrum, compound **3** showed characteristic band for C≡N at 2233 cm^{-1}, and the disappearance of the OH group was observed. In ^{1}H-NMR spectrum of compound **3**, OH group of compound **1** disappeared as expected. ^{1}H-NMR spectrum of **3** showed new signals at δ = 8.33 (d, 1H, =C-H), 8.19-7.97 (m, 16H, Ar-H) and 2.32 (d, 3H, CH_3). The ^{13}C-NMR spectrum of compound **3** indicated the presence of nitrile carbon atoms with signals at δ=115.99-115.06 ppm. The MALDI-TOF mass spectrum of compound **3,** which showed a peak at m/z = 481,37 $[M+H]^+$, supports the proposed formula for this compound (Fig. S1, SI).

The metal-free phthalocyanine **4** and the metallophthalocyanines **5-8** were prepared with phthalonitrile derivative **3** and corresponding dry metal salts [$Zn(CH_3COO)_2$, $Ti(OBu)_4$, $NiCl_2$ and $CoCl_2$] in the presence of a few drops of 1,8-diazabicyclo[5.4.0]undec-7-ene (DBU) by heating under reflux temperature in dry n-amyl alcohol for 16 h, 16 h, 12 h, 12 h and 12 h, respectively. After cyclotetramerization of dinitrile **3** to the phthalocyanines, the C≡N vibration around 2233 cm^{-1} disappeared. IR spectra of phthalocyanines **4-8** were very similar. Additionally, IR spectrum of phthalocyanine **4** showed NH stretching vibration at 3292 cm^{-1}, which is characteristic for metal-free Pcs. However, in the ^{1}H-NMR spectrum, the NH protons of compound **4** could not be observed because of the probable strong aggregation of the molecules [13]. The ^{1}H-NMR spectrum of metal-free **4** showed characteristic protons between 8.31-2.32 ppm. The MALDI-TOF mass spectrum of compound **4,** which showed a peak at m/z=986 $[M-4(C_{15}H_{12}N_3)]^+$, supports the proposed formula for this compound.

The IR spectra of **ZnPc**, **TiOPc, NiPc** and **CoPc** were also very similar to that of the precursor **3**. In the IR spectra of the metallophthalocyanines **5-8**, cyclotetramerization of compound **3** was confirmed by the disappearance of the sharp C≡N stretching vibration at 2233 cm^{-1}. The ^{1}H-NMR spectrum of compound **8** could not be determined because of the paramagnetic nature [14]. In the MALDI-TOF mass spectrum of Zn, Ti, Ni, Co phthalocyanines, the presence of molecular ion peaks at m/z = 1050.38 $[M-4(C_{15}H_{12}N_3)]^+$, 1049.56 $[M-4(C_{15}H_{12}N_3)]^+$, 1042.78 $[M-4(C_{15}H_{12}N_3)]^+$ and 1044.25 $[M-4(C_{15}H_{12}N_3)]^+$, respectively, confirmed the proposed structures (Figure S3- S5, SI).

The UV- Vis spectra of the metal-free Pc **4** and MPcs **5-8** show typical electronic spectra with two strong absorption regions. The band in the visible region at 600-700 nm (Q band) is the one of them, and the other one is in the UV region at about 300-500 nm (B band), both correlate to transitions from π-HOMO to π*-LUMO energy levels [15-16]. The ground state electronic spectra of the compounds showed characteristic absorptions in the Q band region at 698/664 nm for compound **4**, 677 nm for compound **5**, 698 nm for compound **6**, 668 nm for compound **7**, and 670 nm for compound **8** in $CHCl_3$. B band absorptions of the metal-free and metallophthalocyanines **4-8** were observed at 342, 351, 349, 334, and 346 nm, respectively (Fig. 2).

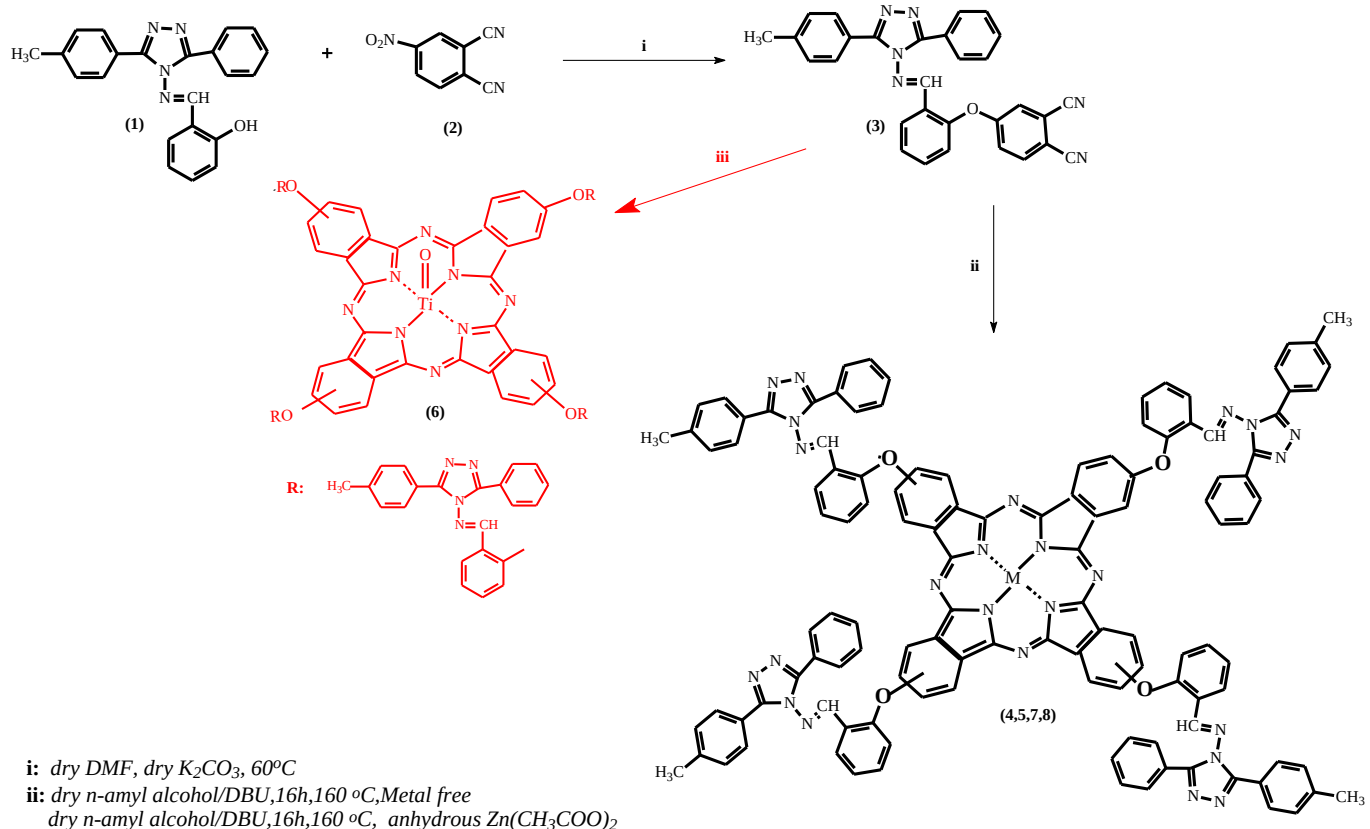

Compound	4	5	7	8
M	2H	Zn(II)	Ni(II)	Co(II)

i: *dry DMF, dry K_2CO_3, 60^{o}C*
ii: *dry n-amyl alcohol/DBU,16h,160 ^{o}C,Metal free*
dry n-amyl alcohol/DBU,16h,160 ^{o}C, anhydrous $Zn(CH_3COO)_2$
dry n-amyl alcohol/DBU,12h,160 ^{o}C, anhydrousdry $NiCl_2$
dry n-amyl alcohol/DBU,12h,160 ^{o}C, anhydrous $CoCl_2$
iii: *dry n-amyl alcohol/DBU,12h,160 ^{o}C, anhydrous $Ti(OBu)_4$*

Fig. 1. The synthesis route of new compounds

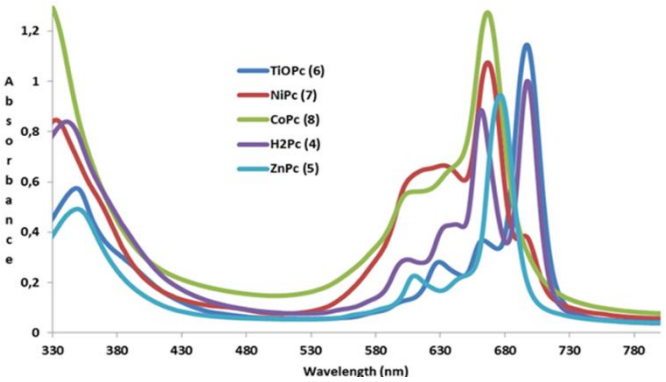

Fig 2. UV-Vis absorption spectra of compounds **4**, **5, 6, 7** and **8** in $CHCl_3$ at $1x10^{-5}$ mol.L^{-1}

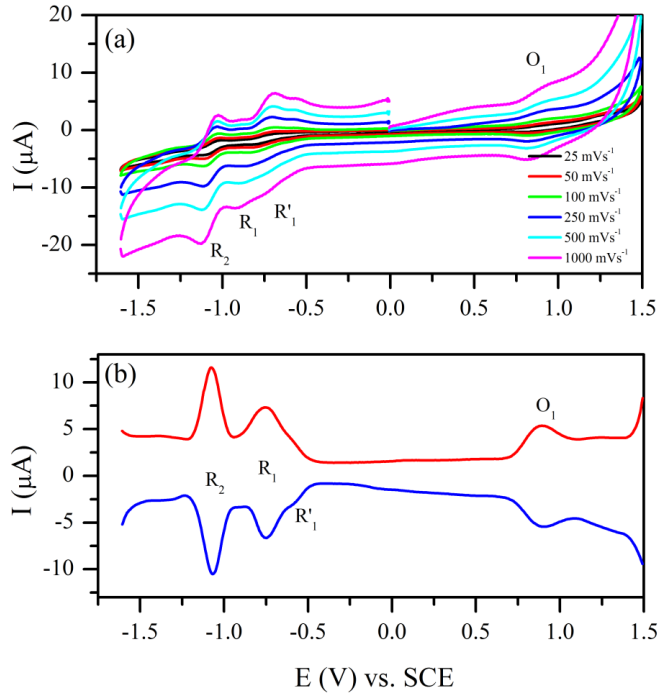

Fig 3. (**a**) CVs of **NiPc** at various scan rates and (**b**) SWVs of **NiPc** recorded at 0.100 Vs^{-1} scan rate on a Pt working electrode in DCM/TBAP.

3.3. Voltammetric measurements

CV and SWV responses of the MPc complexes were carried out in DCM/TBAP electrolyte system on a Pt working electrode to determine their electrochemical properties. CV and SWVs were analyzed, and the results, the assignments of the redox couples and estimated electrochemical parameters including the half-wave peak potentials ($E_{1/2}$), ratio of anodic to cathodic peak currents ($I_{p,a}/I_{p,c}$), peak to peak potential separations (ΔE_p), peak width (ΔE_p), dE_p/dv values, and difference between the first oxidation and reduction processes ($\Delta E_{1/2}$) are given in Table. Among the complexes, **NiPc** and **ZnPc** have redox inactive metal centers, thus redox behaviors of these complexes are different than those of **CoPc** and **TiOPc**, since **CoPc** and **TiOPc** give metal based reduction reactions due to the redox activity of the metal centers of these complexes. The general similarity of the complexes is aggregation behaviors of the complexes, which is reflected with the splitting of the redox processes due to the existence of equilibrium between aggregated and disaggregated species.

Fig. 3 shows the CV and SWV responses of **NiPc** recorded in DCM/TBAP electrolyte system on a Pt working electrode. **NiPc** gave two reduction processes, $\mathbf{R_1}$ at -0.74 V (ΔE_p=80 mV and $I_{p,a}/I_{p,c}$=1.26) and $\mathbf{R_2}$ at -1.07 V(ΔE_p=62 mV and $I_{p,a}/I_{p,c}$=0.95). First reduction reaction $\mathbf{R_1}$ was complicated with a shoulder wave $\mathbf{R'_1}$ (at -0.59 V), which was assigned to the reduction of the aggregated species. Splitting of the first reduction reaction decreases the chemical and electrochemical reversibility of the process. The first reduction reaction peaks were broader and had smaller peak currents than those of the second ones. These behaviors were resulted from the aggregation of the complex. After the $\mathbf{R_1}$ couple aggregated species turned into monomeric ones, which gave higher peak currents due to the increase in the concentration of the monomeric ones, the second reduction couple of **NiPc** was electrochemically reversible at all scan rates with respect to ΔE_p, $E_{p/2}$, dE_p/dv and $I_{p,a}/I_{p,c}$ values. The process was also chemically reversible and diffusion controlled with respect to [$I_p \alpha v^{1/2}$] and $I_{p,a}/I_{p,c}$ values [17]. **NiPc** gave an oxidation reaction, $\mathbf{O_1}$ at 0.87 V (ΔE_p=90 mV and $I_{p,a}/I_{p,c}$=1.23) in addition to the reduction reactions. However the $\mathbf{O_1}$ process gave broad waves with small peak currents. This different behavior may be due to the aggregation of the complex. $\Delta E_{1/2}$ (1.46 V) and $\Delta E_{1/2(R1\text{-}R2)}$ (0.33 V) values of **NiPc** were in agreement with the similar complexes in the literature. It is well known that MPcs that have redox inactive metal center generally give a HOMO-LUMO gap ($\Delta E_{1/2}$) between 1.40 and 1.70 V. These type complexes give first two reduction reactions after ca. -0.60 V versus SCE with about 0.30 V potential differences between these two processes ($\Delta E_{1/2(R1\text{-}R2)}$).

Table. Voltammetric data of the complexes. All voltammetric data were given versus SCE.

Complexes	Redox processes	[a] $E_{1/2}$ (V)	[b] ΔE_p (mV)	[c] $I_{p,a}/I_{p,c}$	[d] $\Delta E_{1/2}$
NiPc	$[Ni^{II}Pc^{2-}] / [Ni^{II}Pc^{1-}]^{+1}$	0.87	90	1.23	1.46
	$[Ni^{II}Pc^{2-}] / [Ni^{II}Pc^{3-}]^{-1}$	-0.74 (-0.59)[e]	80	1.26	
	$[Ni^{II}Pc^{3-}]^{-1} / [Ni^{II}Pc^{4-}]^{-2}$	-1.07	62	0.95	
ZnPc	$[Zn^{II}Pc^{2}] / [Zn^{II}Pc^{1-}]^{+1}$	0.79 (0.62)[e]	…	0.94	1.49
	$[Zn^{II}Pc^{2}] / [Zn^{II}Pc^{3-}]^{-1}$	-0.87	61	0.94	
	$[Zn^{II}Pc^{3-}]^{-1} / [Zn^{II}Pc^{4-}]^{-2}$	-1.18	120	0.79	
CoPc	$[Co^{II}Pc^{1-}]^{+1} / [Co^{III}Pc^{1-}]^{+2}$	0.98 (1.13 [e]	65	0.83	1.16
	$[Co^{II}Pc^{2-}] / [Co^{II}Pc^{1-}]^{+1}$	0.69 (0.83)	62	0.90	
	$[Co^{II}Pc^{2-}] / [Co^{I}Pc^{2-}]^{-1}$	-0.47 (-0.91)[e]	200	0.85	
	$[Co^{I}Pc^{2-}]^{-1} / [Co^{I}Pc^{4-}]^{-2}$	-1.28	90	0.72	
TiOPc	$[Ti^{IV}OPc^{2-}] / [Ti^{IV}OPc^{1-}]^{+1}$	0.90	120	0.86	1.45
	$[Ti^{IV}OPc^{2-}] / [Ti^{IV}OPc^{3-}]^{-1}$	-0.55	61	0.96	
	$[Ti^{IV}OPc^{3-}]^{-1} / [Ti^{III}OPc^{3-}]^{-2}$	-0.74	-	-	
	$[Ti^{III}OPc^{3-}]^{-2} / [Ti^{III}OPc^{4-}]^{-3}$	-0.92	63	0.87	
	$[Ti^{III}OPc^{4-}]^{-3} / [Ti^{II}OPc^{4-}]^{-4}$	-1.08	-	-	

a: $E_{1/2}$ values ((E_{pa}+E_{pc})/2) were given versus SCE) at 0.100 Vs^{-1} scan rate. b: ΔE_p= E_{pa}-E_{pc}. c: $I_{p,a}/I_{p,c}$ for reduction ,$I_{p,c}/I_{p,a}$for oxidation processes. d: $\Delta E_{1/2}$ = $E_{1/2}$ (first oxidation)- $E_{1/2}$ (first reduction). e: $E_p$value of aggregated species given in parentheses.

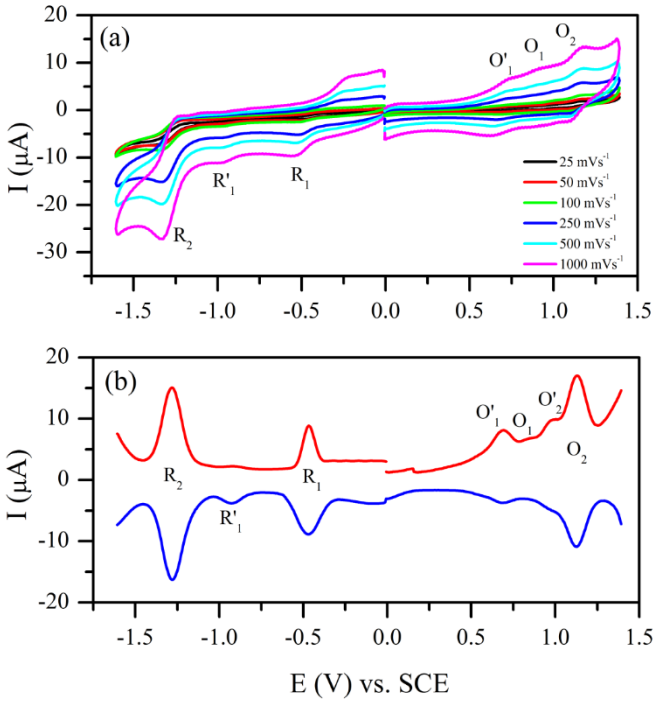

Fig. 4. (**a**) CVs of **CoPc** at various scan rates and (**b**) SWVs of **CoPc** recorded at 0.100 Vs^{-1} scan rate on a Pt working electrode in DCM/TBAP.

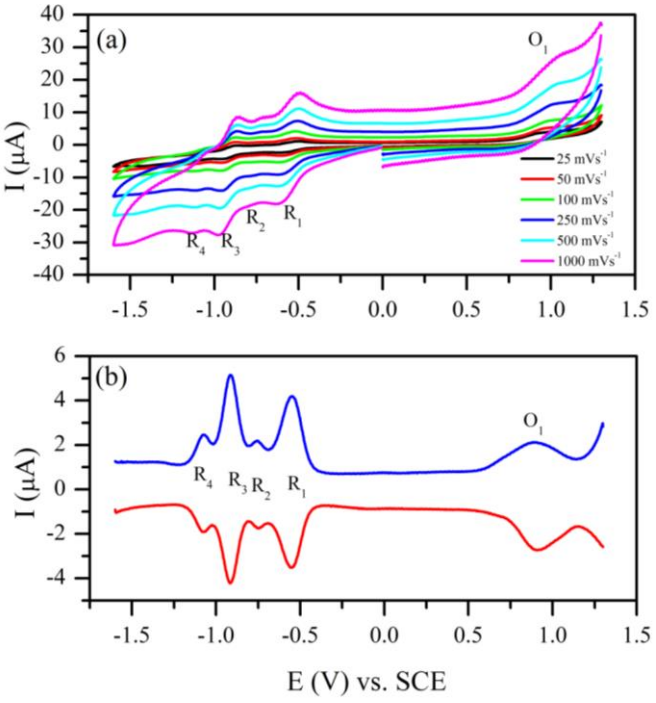

Fig. 5. (**a**) CVs of **TiOPc** at various scan rates and (**b**) SWVs of **TiOPc** recorded at 0.100 Vs^{-1} scan rate on a Pt working electrode in DCM/TBAP.

Fig. S6 (SI) represents the CV and SWV responses of **ZnPc**, which illustrated similar voltammetric responses with those of **NiPc.** Two reduction processes, $\mathbf{R_1}$ at -0.87 V (ΔE_p=61 mV and $I_{p,a}/I_{p,c}$=0.94) and $\mathbf{R_2}$ at -1.18 V(ΔE_p=120 mV and $I_{p,a}/I_{p,c}$=0.79) and one split oxidation process ($\mathbf{O'_1}$ at 0.62 V and $\mathbf{O_1}$ at 0.79 V) were observed with **ZnPc**. Main difference between these two complexes was in their aggregation tendencies. While aggregation effect was clearly pronounced on the first reduction reaction of **NiPc**, the aggregation wave $\mathbf{R'_1}$ that was recorded before $\mathbf{R_1}$ was almost invisible for **ZnPc**. Thus, the $\mathbf{R_1}$ of **ZnPc** was almost reversible at all scan rates chemically and electrochemically. On the contrary, effect of aggregation was more distinctive on the oxidation reaction of **ZnPc**. The oxidation reaction of **ZnPc** splitted into two waves, $\mathbf{O'_1}$ assigned to the aggregated species and $\mathbf{O_1}$ assigned to the monomeric species. Concentration effect on the SWVs of **ZnPc** illustrated the aggregation reaction of the complex more clearly as shown in Fig. S6b (SI). $\Delta E_{1/2}$ (1.49 V) and $\Delta E_{1/2(R1\text{-}R2)}$ (0.31 V) values of **ZnPc** were in agreement with those of **NiPc** and the similar complexes in the literature [18-22]. When we compared $\Delta E_{1/2}$ values, it is clear that redox reaction of **ZnPc** shifts about 0.130 V towards negative potentials with respect to **NiPc**, due to the effective nuclear charge differences between Zn^{II} and Ni^{II} metal centers.

Electroactive nature of the Co^{II} center of **CoPc** differentiates the redox responses of the complex from those of **NiPc** and **ZnPc**. **CoPc** gave a metal based reduction reaction $\mathbf{R_1}$ at almost -0.47 V in addition to the Pc ring based reduction reaction at -1.28 V ($\mathbf{R_2}$) (Fig. 4). During the anodic potential scans **CoPc** illustrated two oxidation processes, $\mathbf{O_1}$ at 0.69 V and $\mathbf{O_2}$ at 1.13 V. Due to the aggregation of the complex, a reduction wave $\mathbf{R'_1}$ at -0.92 V and oxidation waves $\mathbf{O'_1}$ and $\mathbf{O'_2}$ were also recorded. The first reduction reaction $\mathbf{R_1}$ of **CoPc** deviated from reversibility at even slow scan rates with respect to ΔE_p and $I_{p,a}/I_{p,c}$ values (ΔE_p=200 mV and $I_{p,a}/I_{p,c}$=0.85 at 0.025 Vs^{-1} scan rate). Moreover, $\mathbf{R_2}$ of **CoPc** had irreversible character electrochemically, and the oxidation processes had reversible character electrochemically but irreversible character chemically. SWVs of the complex illustrated these analyses results more clearly as shown in Fig. 4b. For instance, different peak current values of $\mathbf{R_1}$ couple illustrated the chemical irreversibility of the process and presence of aggregation-disaggregation equilibrium coupled with this process. However, $\mathbf{R_2}$ process seemed as a reversible one chemically with respect to peak current ratio of the waves that were recorded with SWV.

TiOPc shows completely different electrochemical responses from all of the other complexes. Though two reduction reactions were observed with **NiPc, ZnPc** and **CoPc**, **TiOPc** presented four reduction and one oxidation reactions (Fig. 5). While two reduction reactions ($\mathbf{R_1}$ and $\mathbf{R_2}$) had expected peak currents, other reduction couples ($\mathbf{R_3}$ and $\mathbf{R_4}$) had five-fold smaller peak currents than $\mathbf{R_1}$ and $\mathbf{R_2}$. These different peak currents may arise due to different number of transferred electrons and/or different rates of electron transfer reactions. It is well documented that electron transferring more than one is uncommon for MPc complexes [23]. Thus, all of these redox processes should be one-electron processes. However, peak current differences cause serious doubt about the number of electrons transferred. To clarify this, CPC analyses of these peaks were performed. When the **TiOPc** solution was electrolyzed at -0.60 V, the number of electron was found to be one for the first reduction peak. Electrolysis of a fresh **TiOPc** solution at -1.50 V gave the total number of electrons that were transferred during reduction reactions as four. These CPC measurements indicated one electron character of each reduction reaction, even though they have different peak currents. These uncommon peak currents may be due to different electron transfer rates of these processes. It is known that $Ti^{IV}O$ center of TiOPc type complexes give metal based reduction reactions in addition to Pc based processes [24-26]. These differently assigned processes may have different electron transfer rates. In situ spectroelectrochemical measurements (given below) were carried out to determine assignments of the redox reactions of **TiOPc**.

3.4. Spectroelectrochemical measurements

In situ spectroelectrochemical measurements were carried out to execute assignments of the redox couples that were recorded in the CVs and SWVs of the complexes. **NiPc** and **ZnPc** complexes have redox inactive metal center; therefore, spectral changes which characterized ring-based reduction reactions were only observed with these complexes. As a representative of these type complexes, in situ spectroelectrochemical and in situ electrocolorimetric analyses results are given in Fig. 6. Fig. 6a shows the in situ UV-Vis spectral changes and in situ recorded chromaticity diagram of **ZnPc** that was recorded during the first reduction process at -1.00 V constant potential application. During this process, while the Q band at 675 nm decreased without shift, new bands were observed at ligand to metal

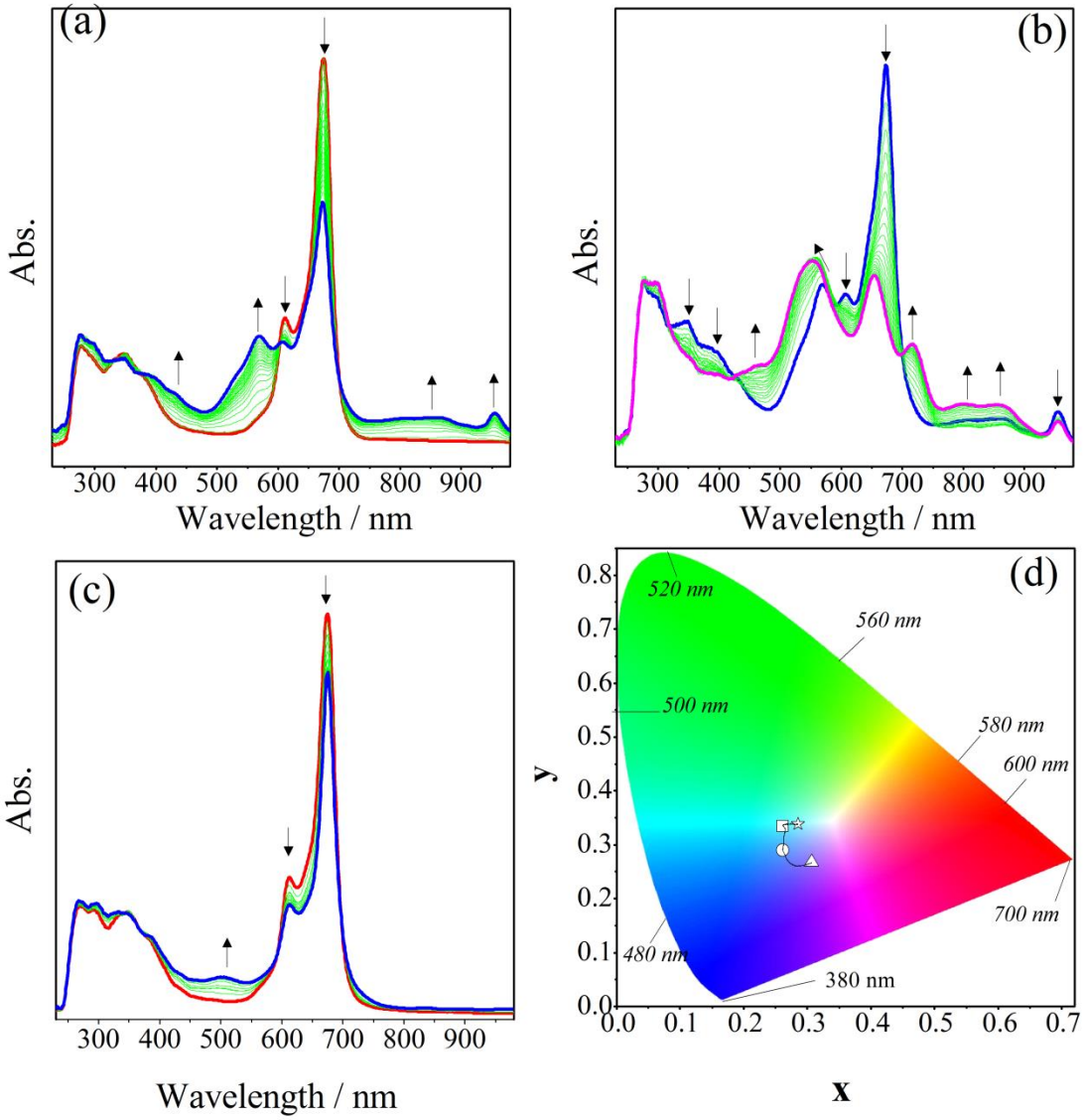

Fig. 6. In-situ UV-Vis spectral changes of **ZnPc** in DCM/TBAP: **a**) E_{app}=-1.00 V, **b**) E_{app}=-1.40 V, **c**) E_{app}=1.20 V, **d**) chromaticity diagram (each symbol represents the color of electro-generated species; □: $[Zn^{II}Pc^{-2}]$, ○:$[Zn^{II}Pc^{-3}]^{-1}$; △: $[Zn^{II}Pc^{-4}]^{-2}$; ☆: $[Zn^{II}Pc^{-1}]^{+1}$.

charge transfer region (LMCT) (568, 865, and 956 nm). Well-defined isosbestic points were observed at 370, 600, and 700 nm in the spectra which indicated presence of one reduced species during the first reduction reaction. These spectral changes characterized the formation of monoanionic $[Zn^{II}Pc^{-3}]^{1-}$ species from the neutral $[Zn^{II}Pc^{-2}]$ [19-22]. While the neutral $[Zn^{II}Pc^{-2}]$ had cyan color (x=0.2608 and y=0.3349), its color changed to blue (x=0.261 and y=0.2898) after the first reduction process (Fig. 6d). Under -1.40 V potential application, the Q band continued to decrease and the band at 570 nm shifted to 552 nm with an increase. At the same time, while the band at 956 nm decreased, a new band enhanced at 718 nm. These spectral changes were in consistent with the second reduction reaction of MPc type complexes and were easily assigned to $Zn^{II}Pc^{-3}]^{1-}$/ $Zn^{II}Pc^{-4}]^{2-}$ [24-26]. These spectral changes caused to color changes from blue to purple (x=0.307 and y=0.267) as shown in the chromaticity diagram (Fig. 6b). During the oxidation of **ZnPc**, any significant spectral changes could not be observed. While the Q bands decreased slightly, a new band started to enhance at 505 nm (Fig. 6c).

Fig. S7 (SI) represents in situ spectroelectrochemical and in situ electrocolorimetric analysis results of **CoPc**. **CoPc** has redox active Co^{II} center; therefore, it gave more different spectral changes than those of **ZnPc** and **NiPc**. In our previous papers [24-26], we reported the spectroelectrochemical behaviors of various **CoPc** complexes. It has been represented in our previous papers that **CoPc** complexes illustrate characteristic spectral changes for the metal based and ring based electron transfer reactions [27-30]. The characteristic spectral changes that were recorded during the metal-based reduction reaction were shifting of the Q band to longer wavelengths and observation of a new intense band between 400 and 550 nm. Surprisingly, **CoPc** that was studied here showed more different spectral changes than those of the similar **CoPc** complexes in the literature during the first reduction reaction as shown in Fig. S7a (SI). Prior to potential application, the Q band at 665 nm had a shoulder at 612 nm due to the aggregation of the complex. Under -0.70 V potential application, two distinct spectral changes were observed. First of all, common spectral changes that were assigned to $[Co^{II}Pc^{-2}]/[Co^{I}Pc^{-2}]^{1-}$ process started to occur as shown in Fig. S7a (SI) inset. During this process, the Q band at 665 nm decreased, and a new band started to increase at 702 nm, and a new band was observed at 465 nm. These spectral changes illustrated reduction of the monomeric **CoPc** species, since the band at 612 nm, which was assigned to the aggregated species, stayed stable without any significant changes. Then the trend of the previous spectral behaviors started to change. As the band at 465 nm continued to increase, the Q band at 665 nm increased in absorption intensity (Fig. S7a, SI). These spectral changes indicated the presence of aggregation-disaggregation equilibrium and turned the aggregated

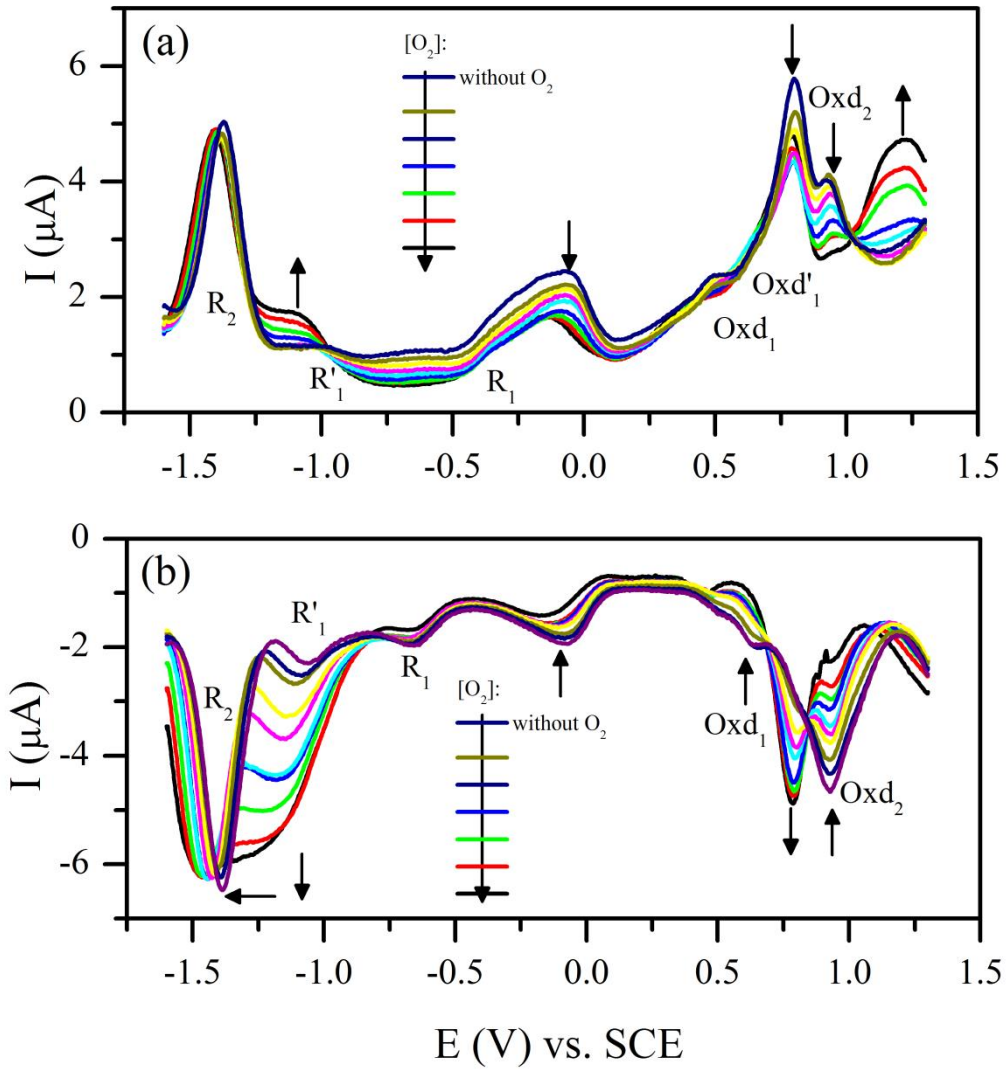

Fig. 7. SWV responses of **CoPc** recorded at 0.100 Vs^{-1} scan rate on a Pt working electrode in DCM/TBAP which is gradually bubbled with O_2 gas.

species into monomeric one due to the reduction reaction. At the end of the first reduction reaction, both the aggregated and monomeric species reduced to $[Co^{I}Pc^{-2}]^{1-}$ species. At the end of this reaction, greenish blue color (x=0.2388 and y=0.3137) of the complex turned into green color (x=0.3012 and y=0.3755) as shown in the chromaticity diagram. During the second reduction reaction, the Q band decreased in intensity, while the intensity of the region at around 540 nm increased. A light yellow color (x=0.3676 and y=0.3424) was observed at the end of the second reduction reaction. These spectral changes were characteristic changes for a Pc-ring based reduction reaction (Fig. S7b, SI) [27-30]. Fig. S7c (SI) represents the Pc ring based oxidation of **CoPc** under the application of constant 0.80 V potential. During this process, the Q band decreased without a shift, while new bands were observed at 530 and 740 nm. This process gave clear isosbestic points at 485 and 704 nm and a color change from greenish blue to purple (x=0.317 and y=0.300).

Fig. S8 (SI) represents in situ spectroelectrochemical and in situ electrocolorimetric analysis results of **TiOPc**. **TiOPc** has redox active $Ti^{IV}O$ center, thus it gives characteristic spectral changes for metal-based electron transfer reactions in addition to ligand-based redox reactions. In our previous papers we illustrated that while peak assignments of **CoPc**, **ZnPc**, and **NiPc** did not change with redox inactive substituents, peak assignments of **TiOPc** type complexes altered with the substituents environment. For instance, while **TiOPc** which bears octakis(2-dimethylaminoethylsulfanyl moieties [31] has a metal-ring-metal-ring assignment, **TiOPc** which bears tetra[4-(thiophen-3-yl)-phenoxy] moieties [30] has a metal- metal-ring-ring assignment. In contrast, **TiOPc** was studied here showed a ring-metal-ring–metal assignment. Under -0.60 V potential application, decrease of the Q band at 696 nm without shifting and observation of a new band at 712 nm were characteristic changes for a ring based redox reaction and assigned to $[TiO^{IV}Pc^{-2}]$/ $[TiO^{IV}Pc^{-3}]^{1-}$ process [30-31] (Fig. S8a, SI). Clear isosbestic points at 408, 578, and 740 nm and color change from bluish green (x= 0.2863 and y= 0.3551) to light green (x=0.334 and y=0.341) were observed during this process. Second reduction reaction of **TiOPc** (**R_2**) was a metal-based process ($[TiO^{IV}Pc^{-3}]^{1-}$/ $[TiO^{III}Pc^{-3}]^{2-}$) [32-33], since the Q band of the complex shifted from 696 to 674 nm while a new band was observed at 920 nm (Fig. S8b, SI). Simultaneously, the band at 712 nm disappeared at the end of the second reduction reaction. Shifting of the Q band and observation of a new band at the metal to charge transfer (MLCT) region are characteristic changes for a metal based reduction reaction of MPc type complexes. Light green of the $[TiO^{IV}Pc^{-3}]^{1-}$ species turned into light yellow color (x=0.341 and y=0.344) after the second reduction reaction as shown in the chromaticity diagram given in Fig. S8d (SI). Similarly third reduction reaction **R_3** is a Pc ring-based reduction reaction ($[TiO^{III}Pc^{-3}]^{2-}$ /$[TiO^{III}Pc^{-4}]^{3-}$) [15, 16, 28-30]. During this reaction, the Q band decreased in intensity, while two new bands were observed at 600 and 752 nm (Fig. S8b inset, SI). Light yellow color of the $[TiO^{III}Pc^{-3}]^{2-}$ species turned into red color (x=0.4078 and y=0.3374) after the third reduction. Under -1.20 V potential application (**R_4**), the Q band at 674 nm shifted to 634 nm and a new band was observed at 538 nm (Fig. S8c, SI). These changes were assigned easily to $[TiO^{III}Pc^{-4}]^{3-}$/

$[TiO^{II}Pc^{-4}]^{4-}$. At the end of the reduction reactions of **TiOPc**, a pink color (x= 0.3904 and y= 0.302) was observed as shown in the chromaticity diagram. **TiOPc** decomposed during the oxidation reaction under constant potential application, since all bands decreased in absorption intensity without giving isosbestic points as shown in Fig. S8a inset (SI).

3.5. Electrochemical oxygen sensing measurements

During the voltammetric and in situ spectroelectrochemical measurements, it was noticed that penetration of molecular oxygen in the electrolytes alters the redox responses of MPcs due to the interaction between O_2 and MPcs. Due to this interaction, MPcs were used as electrocatalyst for oxygen reduction reaction in different media. In our previous papers, we reported that MPcs that had redox active metal centers, such as **CoPc**, **MnPc** and **TiOPc**, catalyzed oxygen reduction reaction electrochemically (ORR) [32-34]. It was also introduced that tailoring the MPcs with different substituents alters the catalytic activities of MPcs. Here we represented the electrocatalytic activity of MPcs that have substituents and substituent effects on the interaction between MPcs and molecular oxygen. During the electrocatalytic ORR measurements, we noticed that **CoPc** behaved as an electrosensor for molecular oxygen. **CoPc** represented similar SWV responses with those reported in our previous papers. This SWV responses could be briefly explained as that; one electron reduced form of **CoPc** interact with O_2, and this interaction decreased the ORR potential and altered the second reduction reaction of **CoPc**. These voltammetric responses were well seen in Fig. 7. During the gradual increase of O_2 in DCM/TBAP electrolyte, while the $\mathbf{R_1}$ peak slightly decreased in current intensity, O_2 gave ORR at -1.25 V. Moreover $\mathbf{R_2}$ peak of **CoPc** at -1.50 V shifted to the negative potentials gradually. These voltammetric data supported the electrocatalytic activity of **CoPc** for the ORR. In addition to the electrocatalytic activity, SWV responses of **CoPc** recorded at the anodic potentials of DCM/TBAP electrolyte during the gradual O_2 addition indicate the electrosensing activity of the complex. Without O_2, **CoPc** gave two oxidation couples, Oxd_1 at 1.0 V assigned to the Pc based oxidation and Oxd_2 at 1.20 V assigned to the metal based oxidation process of **CoPc**. When O_2 concentration increased gradually, both the anodic and cathodic peaks of Oxd_2 couple decreased and a new couple was recorded at just positive side of the Oxd_2 couple. Finally, Oxd_2 couple shifted form 1.20 V to 1.40 V due to the interaction with O_2. These voltammetric data indicated that **CoPc** interacts with O_2, and this interaction shifted the metal based oxidation couple of the **CoPc** to the positive potentials as a result of increasing O_2 concentration. These voltammetric results represented usability of **CoPc** as an oxygen sensor. Observation of a new couple at 1.40 V showed selectivity of the complex for O_2 and the peak current that increased in this new couple and peak current that decreased in O_2 couple could be used to determine the amount of O_2 in the solution.

O_2 interaction of **ZnPc**, **NiPc**, and **TiOPc** were also tested. While **ZnPc** and **NiPc** did not interact with oxygen, the reduction processes of **TiOPc** altered due to the interaction with O_2 as shown in Fig. S9 (SI). With gradual increase in O_2 concentration, the metal-based reduction peaks ($\mathbf{R_2}$ and $\mathbf{R_4}$) of **TiOPc** disappeared immediately, while the peaks of the first Pc based reduction couple $\mathbf{R_1}$ decreased slightly in current intensity. Moreover, the second Pc based reduction peaks $\mathbf{R_3}$ shifted to the negative potentials gradually. At the same time, ORR peaks were observed at -1.15 V. These voltammetric data indicated that $Ti^{IV}O$ center of the **TiOPc** interacts with O_2, and this interaction catalyzed the ORR. While oxidation processes of **CoPc** were altered with increasing O_2 concentration, oxidation peaks of **TiOPc** did not change. Consequently, while **CoPc** and **TiOPc** behaved as ORR electrocatalysts, only **CoPc** among the complexes that were studied here could be used as an oxygen sensor.

3.6. Aggregation studies

In UV–Vis spectra, the formation of the phthalocyanine structures are one of the most important indicators for Pcs. The metal-free Pc (**4**) and MPcs (**5-8**) showed two strong absorption regions in their electronic spectra. One of them is in UV region at about 300–500 nm (B band) and the other one is in the visible region at 600–800 nm (Q band) [33]. The Q band absorptions of compound **4** in chloform ($CHCl_3$) at λ=698, 664 nm and 644, 607 nm as shoulders, and the other absorption (B band) at 342 nm are in agreement with the results that were obtained for previous phthalocyanines [35]. As can be seen in the spectrum (Fig. 2), the splitting of Q band absorption of **4** to Qx and Qy bands can be attributed to the fact that the symmetry of metal-free phthalocyanine is nondegenerate (D_{2h}), but for metallated species, the Q band is observed as one peak due to a degenerate D_{4h} symmetry [34, 35].

The UV-Vis absorption spectra of metallophthalocyanines **5-8** are given in Fig. 2. These compounds showed the expected absorptions at the main peaks of the Q and B bands that appear at λ=677-611 nm (corresponding to degenerate D_{4h} symmetry), 351 nm (corresponding to B region) for Zn (II), 698, 666, 631 and 349 nm for Ti(IV), 668, 621 and 334 nm for Ni(II), and 670, 640 and 346 nm for Co(II) (Fig. 2), respectively. These results are typical for metal complexes of substituted and unsubstituted Pcs with D_{4h} symmetry [31,34-37]. The absorption spectra of **5-8** in $CHCl_3$ indicated that all compounds existed mainly as a monomeric species.

Aggregation depends on the nature of solvent, concentration, temperature, coordinated metal ions, and nature of the substituents. The aggregation of the phthalocyanines is usually indicated by the hypsochromic shift of the Q-band at 700 nm and gradual broadening of this region in hypochromic fashion [37]. In this study, the aggregation behaviors of the phthalocyanine complexes **4** and **5** were investigated in different solvents and different concentrations by UV-Vis spectroscopy (Figs. S10 and S11, SI). The aggregation behavior of metal-free **4** and metallophthalocyanine **5** were studied at different concentrations in $CHCl_3$ as detection of the aggregation depends on concentration. The studied phthalocyanines (**4** and **5**) did not show any aggregation at $2x10^{-6}$ M and $12x10^{-6}$ M concentration ranges in $CHCl_3$ (Figs. S10a and S11a, SI) and they showed monomeric behavior.

Organic solvents are known to reduce aggregation but aqueous solvents result in highly aggregated complexes [38]. Especially, the absorption intensities of Q bands are changed by the solvent markedly. To investigate the effect of the solvents on the aggregation behavior of **4** and **5**, we measured the absorptions of **4** and **5** in different solvents at $1.2\ x10^{-5}$ and $8x10^{-5}$ $mol.L^{-1}$, respectively. For example, in Fig. S10b (SI), for metal-free phthalocyanine **4**, Q bands were very sharp intense in $CHCl_3$, whereas Q band decreased in THF, DMF, CH_2Cl_2 DMSO, EtOAc and acetone remarkably. Therefore, metal-free phthalocyanine **4** did not show any aggregation in $CHCl_3$, but it showed aggregation in especially DMSO, EtOAc and acetone. In Fig. S11b (SI), zinc phthalocyanine **5** did not show any aggregation in THF and acetone.

4. Conclusion

In this work, the synthesis of new soluble metal-free **4** and metallophthalocyanine (**Zn**, **Ti**, **Ni** and **Co**) **5-8** compounds that bearing 1,2,4-triazole moieties on peripheral positions were synthesized, and these new compounds were characterized by IR, ^{1}H-NMR, ^{13}C-NMR, UV-Vis (for phthalocyanines) and MALDI-MS spectra. Solvent effect (DMF, DMSO, THF, CH_3COCH_3, $CHCl_3$, CH_2Cl_2 and EtOAc) on the aggregation of these tetra-substituted phthalocyanines was determined. While metal-free phthalocyanine **4** was found to be monomeric in only $CHCl_3$, zinc(II) phthalocyanine **5** in THF and acetone. Electrochemical and spectroelectrochemical results of the complexes convey the proposed structure of the complexes. Presence of Co^{II} and $Ti^{IV}O$ metal centers in the core of the Pc ring enhanced the redox richness of the complexes due to the metal based redox processes of **CoPc** and **TiOPc** complexes. Distinct variations between the colors of the electrogenerated species that were recorded with in situ electrocolorimetric measurements indicate their possible application in the display technologies, e.g. electrochromic and data storage application. While the **NiPc** and **ZnPc** complexes did not interact with the molecular oxygen, **CoPc** and **TiOPc** complexes catalyzed ORR. Moreover, **CoPc** behaves as an oxygen sensor.

SUPPORTING INFORMATION

The supplementary material associated with this article is available at http://dergipark.gov.tr/download/article-file/447370.

References

1. McKeown, N. B., Phthalocyanine Materials, (Cambridge University Press, Cambridge, 1998.
2. Liu, H., Shen, Q., Zhang, J., Fu, W., Evaluation of various inverse docking schemes in multiple targets identification, *J. Mol. Graph. Model.* 2010, 29, 326-330.
3. Leznoff, C. C., Lever, A. B. P., Phthalocyanines: properties and applications, New York: VCH Publisher, 1996, 4.
4. Jori, G., Tumour photosensitizers: approaches to enhance the selectivity and efficiency of photodynamic therapy, *J. Photochem. Photobiol B: Biol.* 1996, 36, 87-93.
5. Moser, F. H., Thomas, L. R., Phthalocyanine compound. New York: Reinhold, 1963, 123-1451.
6. Bouvet, M., Phthalocyanine-based field-effect transistors as gas sensors, *Anal. Bioanal. Chem.* 2006, 384, 366-373.
7. Ogunsipe, A., Maree, D., Nyokong, T., Solvent effects on the photochemical and fluorescence properties of zinc phthalocyanine derivatives, *J. Mol. Struct.* 2003, 650, 131-140.
8. Zhou, C. H., Wang, Y., Recent researches in triazole compounds as medicinal drugs, *Curr. Med. Chem.* 2012, 19, 239-280.
9. Barbera, J., Marcos, M., Melendez, E., Ros, B., New liquid crystals: 6-n-alkoxy-3-pyridinecarboxaldehyde derivatives, *J. L. Serrano Mol. Cryst. Liq. Cryst.* 1985, 123, 159-167.
10. Velazquez, S., Alvarez, R., Perez, C., De C. Gago, F., Balzarini, J., Camaraza, M., Regiospecific synthesis and anti-human immunodeficiency virus activity of novel 5-substituted N-alkylcarbamoyl and N,N-dialkyl carbamoyl 1,2,3-triazole-TSAO analogues, *J. Antivir. Chem. Chemoth.* 1998, 9, 481-489.
11. Milaeva, E. R., Speier, G., Lever, A. B. P., Eds.: Leznoff, C. C., Lever, A. B. P. The Phthalocyanines, Properties and Applications, Wiley, 1992, 162–227.
12. Bekircan, O., Kahveci, B., Küçük, M., Synthesis and anticancer evaluation of some new unsymmetrical 3,5-diaryl-4H-1,2,4-triazole derivatives, *Turk. J. Chem*, 2006, 30, 29-40.
13. Demirbas, Ü., Akyüz, D., Akçay, H. T., Barut, B., Koca, A., Kantekin, H., Synthesis, characterization and investigation of electrochemical and spectroelectrochemical properties of non-peripherally tetra-5-methyl-1,3,4-thiadiazole substituted copper(II) iron(II) and oxo-titanium (IV) phthalocyanines, *J. Mol. Struct.* 2017,1144, 112-119.
14. Değirmencioğlu, İ., Er, M., Bayrak, R., Özkaya, A. R., Redox-switchable new phthalocyanines containing hydrazono-thiazole-carboxylate fragments: Synthesis, electrochemical, spectroelectrochemical and electrocolorimetric investigation., *J. Fluores.* 2017, 27, 869-81.
15. Gök, Y., Kantekin, H., Kılıçaslan, M. B., Alp, H., Synthesis and characterization of new metal-free and nickel(II) phthalocyanines containing tetraazatrioxa macrotricyclic moieties, *Dyes Pigm.* 2007, 74, 692-698.
16. Arslanoğlu, Y., Hamuryudan, E., Synthesis and derivatization of near-IR absorbing titanylphthalocyanines with dimethylaminoethylsulfanyl substituents, *Dyes Pigm.* 2007, 75, 150-155.
17. Peter Kissinger, W. R. H., Laboratory Techniques in Electroanalytical Chemistry, 2 ed., Marcel Decker, New York, 1996.
18. Sen, P., Dumludağ, F., Salih, B., Özkaya, A. R., Bekaroğlu, O., Synthesis and electrochemical, electrochromic and electrical properties of novel s-triazine bridged trinuclear Zn (II), Cu (II) and Lu (III) and a tris double-decker Lu (III) phthalocyanines, *Synth. Met.* 2011, 161, 1245-1254.
19. Agboola, B.O., Ozoemena, K.I., Nyokong, T., Electrochemical properties of benzylmercapto and dodecylmercapto tetra substituted nickel phthalocyanine complexes: electrocatalytic oxidation of nitrite, *Electrochim. Acta* 2006, 51, 6470-6478.
20. Aktaş, A., Acar, I., Koca, A., Bıyıklıoğlu, Z., Kantekin, H., Synthesis, characterization, electrochemical and spectroelectrochemical properties of peripherally tetra-substituted metal-free and metallophthalocyanines, *Dyes Pigm.* 2013, 99, 613-619.
21. Alemdar, A., Özkaya, A. R., Bulut, M., Preparation, characterization, electrochemistry and in situ spectroelectrochemistry of novel α-tetra[7-oxo-3-(2-chloro-4-fluorophenyl)coumarin]-substituted metal-free, cobalt and zinc phthalocyanines, *Synth. Met.* 2010, 160, 1556-1565.
22. Perez, E. F., Kubota, L. T., Tanaka, A. A., Neto, G. D., Anodic-oxidation of cysteine catalyzed by nickel tetrasulfonated phthalocyanine immobilized on silica-gel modified with titanium(IV) oxide, *Electrochim. Acta* 1998, 43, 1665-1673.
23. Leznoff, C. C., Lever, A. B. P. Phthalocyanines, Properties and Applications, 4 ed., Wiley-VCH, 1993.
24. Tau, P., Nyokong, T., Electrocatalytic oxidation of nitrite by tetra-substituted oxotitanium(IV) phthalocyanines adsorbed or polymerised on glassy carbon electrode, *J. Electroanal. Chem.* 2007, 611, 10-18.
25. Tau, P., Nyokong, T., Electrochemical characterisation of tetra- and octa-substituted oxo(phthalocyaninato)titanium(IV) complexes., *Electrochim. Acta* 2007, 52, 3641-3650.
26. Demir, F., Erdoğmuş, A., Koca, A., Titanyl phthalocyanines: Electrochemical and spectroelectrochemical characterizations and electrochemical metal ion sensor applications of Langmuir films, *J. Electroanal. Chem.* 2013, 703, 117-125.
27. Arici, M., Arican, D., Uğur, A. L., Erdoğmuş, A., Koca A., Electrochemical and spectroelectrochemical characterization of newly synthesized manganese, cobalt, iron and copper phthalocyanines, *Electrochim. Acta* 2013, 87, 554-566.
28. Arican, D., Aktaş, A., Kantekin, H., Koca, A., Electrochromism of electropolymerized phthalocyanine-tetrahydroquinoline dyads, *J. Electrochem. Soc.* 2014, 161, 670-676.
29. Ortiz, B., Park, S. M., Doddapaneni, N., Electrochemical and spectroelectrochemical studies of cobalt phthalocyanine polymers, *J. Electrochem. Soc.* 1996, 143,1800-1805.
30. Nevin, W. A., Liu, W., Melnik, M., Lever, A. B. P., Spectro electrochemistry of cobalt and iron tetrasulphonated phthalocyanines, *J. Electroanal. Chem.* 1986, 213, 217-234.
31. Koca, A., Arslanoğlu, Y., Hamuryudan, E., Voltammetric and spectroelectrochemical properties of titanylphthalocyanines bearing catecholato and naphthalenediolato moieties, *J. Electroanal. Chem.* 2008, 616, 107-116.
32. Erdoğmuş, A., Koca, A., Uğur, A. L., Erden, I., Synthesis, electrochemical and spectroelectrochemical properties of highly soluble tetra substituted phthalocyanines with [4-(thiophen-3yl)-phenoxy], *Synth. Met.* 2011, 161, 1319-1329.
33. Kamiloğlu, A. A., Acar, I., Bıyıklıoğlu, Z., Novel peripherally tetra substituted metal-free, cobalt(II), copper(II) and manganese(III) phthalocyanines bearing polyethoxy chain attached by 2,6-diphenylphenol groups: synthesis, characterization and their electrochemical studies, *J. Inc. Phenom. Mac. Chem.* 2017, 88 (3-4), 219-228.
34. Özçeşmeci, I., Koca, A., Gül, A., Synthesis and electrochemical and in situ spectroelectrochemical characterization of manganese, vanadyl, and cobalt phthalocyanines with 2-naphthoxy substituents, *Electrochim. Acta* 2011, 56, 5102-5114.
35. Agboola, B., Ozoemena, K. I., Nyokong, T., Synthesis and electrochemical characterisation of benzylmercapto and dodecylmercapto tetra substituted cobalt, iron, and zinc phthalocyanines complexes, *Electrochim. Acta* 2006, 51, 4379-4387.
36. Aktaş, A., Ünlüer, D., Uslu Kobak, R. Z., Acar, I., Düğdü, E., Koca, A., Kantekin, H., 1,2,4-triazole-5(4H)-one based novel peripherally tetra substituted metal-free and metallophthalocyanines: Synthesis, characterization and electrochemical and spectroelectrochemical properties, *Synt. React. Inorg. Metal Org. Nano-Metal Chem.* 2017, 47(6), 830-840.
37. Snow, A. W., Kadish, K. M., Smith, K. M., Guilard, R., The Porphyrin Handbook, in: Phthalocyanine Aggregation, Elsevier Science, Amsterdam, 2003, 17, 129-173.
38. Aydın, M., Alıcı, E. H., Bilgiçli, A. T., Yarasir, M. N., Arabaci, G., Synthesis, characterization, aggregation, fluorescence and antioxidant properties of bearing (4-(methylthio)phenylthio) tetra substituted phthalocyanines, *Inorg. Chim. Acta* 2017, 464, 1-10.